UNIVERSIDAD DE LA FRONTERA
Departamento de Ingeniería de Obras Civiles
Facultad de Ingeniería & Ciencias

RIOC
REVISTA INGENIERÍA DE OBRAS CIVILES



# Water Hammer and Column Separation due to Pump Shutdown.

# Golpe de Ariete y Separación de la Columna Debido al Apagado de la Bomba.

**John Twyman Quilodrán**[1]
[1] Twyman Ingenieros Consultores, Rancagua, Chile.
john@twyman.cl, teléfono: 56-9-89044770

INFORMACIÓN DEL ARTÍCULO

Article history:

Received
22-07-2017
Accepted
15-01-2018
Available
28-02-2018

Keywords:
Cavity Collapse
Cavity Length
Method of Characteristics
Water Column Separation

## Abstract

The phenomenon of water column separation (WCS) and subsequent air cavity collapse (ACC) can significantly increase the maximum pressure, with risk to damage or destroy the pipelines. In this paper, the equations governing this phenomenon by applying the analysis based on the Discrete Vapor-Cavity Model (DVCM) according to the Method of the Characteristics applied on a real pumping system discretized according to the specified time interval are shown. WCS and ACC effects are analyzed when the transient flow is generated by the pumps shutdown located in the system's upstream end. A sensitivity analysis on the main parameters affecting the DVCM model, with special emphasis on the effect of the number of pipe reaches chosen in the discretization and the air cavity length, is performed. It is concluded that the results depend on the initial parameters and the way how the network is discretized.

Historial del artículo:

Recibido
22-07-2017
Aceptado
15-01-2018
Publicado
28-02-2018

Palabras Clave:
Colapso de la cavidad
Discretización de la red
Longitud de la cavidad
Método de las Características
Separación de la columna de agua

## Resumen

El fenómeno de la separación de la columna de agua (SCA) y el posterior colapso de la cavidad de aire (CCA) puede aumentar significativamente la presión máxima, con el riesgo de dañar o destruir las tuberías. En este trabajo se muestran las ecuaciones que rigen estos fenómenos aplicando el análisis basado en el Modelo de Cavidad de Vapor Discreta (MCVD) según el Método de las Características aplicado sobre una impulsión real discretizada utilizando el intervalo de tiempo especificado. Se analizan los efectos de SCA y CCA cuando el flujo transitorio es generado por el apagado de las bombas situadas en el extremo aguas arriba del sistema. Se realiza un análisis de sensibilidad de los principales parámetros que afectan al modelo MCVD, con especial énfasis en el efecto del número de sub-tramos de la discretización y de la longitud de la cavidad de aire. Se concluye que los resultados dependen de los parámetros iniciales y del modo en que está discretizada la red.

## 1. Introduction.

The equations describing water hammer are valid only when the pressure is greater than the liquid's vapor pressure $H_v$ [18]. If the pressure falls below $H_v$ the water column separation occurs in form of cavity (bag) or bubbles, whereupon the fluid becomes a two-phase liquid/liquid or liquid/vapor type (**Figure 1**). Water column separation refers to the breaking of the liquid column in fully filled pipelines. This may occur in a water hammer event when the pressure drops to the vapor pressure at specific locations such as closed ends, high points or knees due to changes in pipe slope [2, 9, 10]. A vapor cavity acts as a low-pressure point, retarding the liquid columns, which finally starts to diminish in size when the liquid columns change flow direction. The collision of two liquid columns, or of one liquid column with a closed end, moving towards the shrinking cavity, may cause a large and nearly instantaneous rise in pressure. In a water hammer event many repetitions of cavity formation and collapse may occur. Some authors mention that the system configuration could be enough to significantly mitigate the effects due to the water column separation (WCS) and cavity collapse, although the depressurization phenomenon and subsequent (WCS) has been shown to have devastating effects on pipe networks [5], especially in systems that have an unfavorable design such as an undulating longitudinal profile with points with higher relative elevation [10]. In less drastic cases, strong pressure surges may cause damage, destruction or deformation to equipment such as pipeline valves, air valves, or other surge protection devices. Sometimes the damage is not realized at the time, but results in intensified corrosion that, combined with repeated transients, may cause the pipeline to collapse in the future [4]. The main difficulty is that accurate estimates are difficult to achieve, particularly because the parameters describing the process are not yet determined during design. Moreover, the vapor cavity collapse cannot be effectively controlled [4].

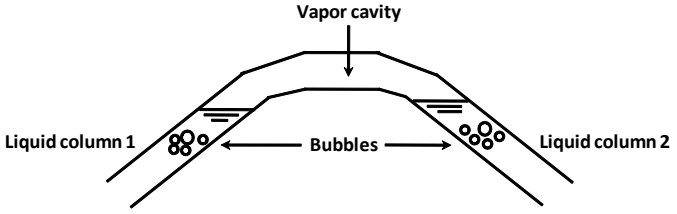


**Figure 1.** Basic scheme of the vapor cavity inside the pipe.

## 2. Material and methods.

A classic example of WCS is the accident that occurred in 1950 at the hydroelectric power plant (HPP) of Oigawa, Japan. During maintenance work, a rapid valve closure caused a severe water hammer which killed three workers. There was a severe drop in pressure produced by the WCS. After that, there was a collapse of a significant pipe portion due to the pressure exerted by the atmosphere. This incident led to pipes redesign able to withstand atmospheric pressure in events where the pressure inside the pipe drops below the vapor pressure. According to Bergant et al. [3], in 1948 Jaeger examined a number of serious accidents due to water hammer in pressurized pipes. Many of the faults detected were related to vibration, resonance or oscillations. Two of the cases analyzed were due to failures attributed to the WCS. In one case, the rapid valve opening produced a negative pressure wave resulting in a WCS effect. Latter, when the liquid columns rejoined, the overpressure generated significant cracks in the affected pipe section. List [8] reviews 10 real cases of systems that suffered the effects of vapor cavity formation, pipeline rupture and air release, all of these effects generated by a rapid drop in pressure. List et al. [9] documented damage resulting from vapor cavity formation and collapse in a 7,010 (m) long, 508-609 (mm) diameter pump discharge pipeline. In 2009 there was a severe water hammer in the Sayano–Shushenskaya plant (Russia) which destroyed the base of turbine 2 (weight: 900 tons) killing 69 workers. The material losses amounted to USD 310 million and a nearby river turned out polluted. Another case occurred in 2011 in Fukushima nuclear plant (Japan), where a fast transient flow ejected radioactive cesium into the atmosphere, contaminating an area as large as the state of Connecticut (USA). Unsteady flow in pipelines can be described by one-dimensional equations of continuity and motion, as follows [18]:

$$H_t + \frac{a^2}{gA} Q_x = 0 \tag{1}$$

$$Q_t + gAH_x + \frac{fQ|Q|}{2DA} = 0 \tag{2}$$

In which $H$ = instantaneous piezometric head, $a$ = wave speed, $g$ = gravitational acceleration, $A$ = pipe cross-sectional area, $Q$ = flow, $f$ = Darcy-Weisbach friction factor and $D$ = pipe diameter. The subscripts $x$ and $t$ denote space and time dimensions, respectively. In this case the adoption of a constant friction factor should not significantly affect the results [12]. Water hammer compatibility equations valid along the positive characteristic $C^+$ ($\frac{dx}{dt} = +a$) and the negative characteristic $C^-$ ($\frac{dx}{dt} = -a$) for the liquid flow are:

$$H = C_P - B_P \cdot Q_u \tag{3}$$

$$H = C_M + B_M \cdot Q \tag{4}$$

Where $B_P$, $B_M$, $C_P$ and $C_M$ are known constants, $Q_u$ = flow upstream of the cavity and $Q$ = flow downstream of the cavity. Both $Q_u$ and $Q$ are within the same computing interval or computational section. Water hammer equations for the liquid flow are valid when the pressure is above the liquid vapor pressure. If the pressure drops below the vapor pressure, column separation occurs either as a discrete cavity or as a vaporous cavitation zone in the liquid [14, 15]. The single-component one-phase flow is transformed into a single-component two-phase flow (liquid/liquid−vapor). Thus the standard water hammer solution is no longer valid. Some of the models to describe the water column separation are the following [14]:

- Discrete Vapor-Cavity Model or DVCM.
- Safwat and van der Polder's model.
- Kot and Youngdahl's model.
- Miwa et al. model.
- Discrete Gas Cavity Model or DGCM.
- Gas Cavity Model.

Adamkowski and Lewandowski [1] proposed a new version of DVCM model which assumes that vaporous zones are in the pipe cross−sectional area. Due to its numerical advantages, the traditional DVCM model [21] is the most widely used method to solve the two-phase flow problem, reason why will be briefly described below. For further details about DVCM and other methods is advisable to consult the references. The DVCM model in standard version has two main advantages:

- It works with MOC in specified time intervals ($\Delta t$).
- It accepts a constant magnitude for wave speed.

The DVCM model allows vapor cavities to form at the MOC computing sections, where the compatibility equations (3) and (4) are applied in the fix and rectangular grid of the specified time interval method. In the interval $\Delta t = \Delta x/a$ ($\Delta t$ = time step, $\Delta x$ = spatial grid size) the continuity equation in the vapor cavity volume is given by:

$$\Delta V_v = \int_{t_i}^{t_f} (Q - Q_u) \cdot dt \qquad (5)$$

In which $\Delta V_v$ = vapor cavity volume, $t_i$ = initial time and $t_f$ = final time. The solution of the continuity equation for the vapor-cavity volume is [1, 2, 14]:

$$(V_v)_{t_f} = (V_v)_{t_i} + \left( \frac{Q_{(t_i)} + Q_{(t_f)} - Q_{u_{(t_i)}} - Q_{u_{(t_f)}}}{2} \right) \cdot \Delta t \qquad (6)$$

The time step in the rectangular grid, based on the Courant condition ($C_n$) for the characteristic lines, is the following:

$$\Delta t = t_f - t_i = \frac{\Delta x}{a} \qquad (7)$$

When the cavity collapses at a section (as a result of a negative cavity volume) the one-phase liquid flow is re-established and equations (3) and (4) are valid. Other models mentioned above work similarly but with some changes or corrections that generate numerical attenuation. Some of them only work in some singular points of the system using average flow values. In a simple pipe network composed of a reservoir (upstream), a pipe of length $L$ and a valve (downstream), the water column separation phenomenon can be described as follows: once the valve is rapidly closed, a positive pressure wave moves toward the reservoir. This wave now negative is reflected from the reservoir, returning to the valve. The return of the wave takes place in a $2(L/a)$ seconds span. The pressure in the valve drops below the vapor pressure, forming an air cavity (vapor) which then collapses, generating an overpressure equal to [21]:

$$\Delta H = \frac{a}{2gA}(Q_u - Q) \qquad (8)$$

In which $\Delta H$ = Joukowsky pressure head rise. Equation (8) shows that $\Delta H$ depends on the both upstream and downstream flow at the time of air cavity collapse [13]. In certain cases $\Delta H$ does not correspond to the expected maximum pressure. Some authors have reported the occurrence of short-duration pressure pulses SDPP [14] that would be generated immediately after the air cavity collapse, and whose magnitude may exceed the pressure given by the Joukowsky formula [19]. Furthermore, it has detected that $\Delta H$ value is very sensitive to $L$ and small variations in $a$, $f$, initial fluid velocity, $D$ and pipe slope. The assumptions related to column separation are [2, 21]:

- The liquid has entrained free gases or dissolved gases that evolve when the pressure drops below saturation pressure.
- The vapor cavity volume must be significantly less than the reach volume in the numerical model.
- The cavity pressure is equal to the vapor pressure.
- Water hammer waves are reflected off the cavity, which is assumed to occupy the total pipe cross-sectional area.
- The vapor cavity does not move.
- Mass and momentum of the cavity vapor are negligible.

- Isothermal conditions in the cavity prevail.
- The vapor condenses completely prior to the instant of liquid columns rejoining or cavity collapse against the boundary.
- The cavities formation has no effect on head losses by $f$.
- The vapor void fraction in the distributed vaporous cavitation zone is much smaller than unity, so the mass and momentum of the bubbles can be neglected.
- The surface tension effect that results in a pressure difference across the vapor bubbles is ignored.
- The liquid and the vapor-bubble velocities in the mixture are the same during vaporous cavitation.
- The vapor bubble is not influenced by the expansion and compression of the neighboring liquid-vapor bubbles.
- The gravity influence on the bubbles is neglected.
- There is an infinitesimal discontinuity width between both the interface of the one-phase fluid (liquid) and the one-component two-phase fluid (homogeneous mixture of liquid and vapor bubbles).
- Increase in temperature across a shock wave front is small and therefore isothermal conditions across the interface prevail.

The SDPP is superimposed to the normal transient pressure due to a sudden valve closure or sudden pump shutdown. It should be emphasized that the maximum pressure head occurrence following the vapor cavity collapse does not occur immediately, it is delayed by between 0 and $2L/a$ (s). The SDPP phenomenon has been widely reported in the literature, such as in Hatcher et al. [7] and Malekpour [11].

**3. Results.**

In the system of **Figure 2**, transient flow is generated by the pumps shutdown located at the upstream end of the pipeline. When pumps are suddenly shutdown, pressure in their discharge side rapidly decreases and a negative pressure wave (which reduces pressure) begins to propagate down the pipeline toward the downstream reservoir. When the negative pressure wave reaches the high point in the pipe, the pressure can drop below atmospheric pressure up to reach the vapor pressure. At this pressure, gas within the liquid is gradually released and the liquid starts to vaporize (column separation). On subsequent cycles of the transient when the pressure recovers, cavity can collapse generating a large pressure surge spike. **Tables 1 and 2** show the pipes and junctions features, respectively, where $\Delta t$ = 0.079586152 (s) and $N$ (number of reaches) and $C_n$ for each pipe is: pipe 1, $N_1$ = 7, $C_n$ = 1.00; pipe 2, $N_2$ = 55, $C_n$ = 1.00; Pipe 3, $N_3$ = 38, $C_n$ = 1.00. The pump data is: number of pumps in parallel (NPP): 4; number of stages for pump: 5; steady-state pump speed: 1,775 (rpm); moment of inertia: 20.017 (kg-m$^2$). The bypass diameter is equal to 0.6096 (m). In order to stop the backflow, the system has a non-return valve located downstream of the pumps set (**Figure 2**). The characteristic curves of the pumps are shown in **Table 3**.

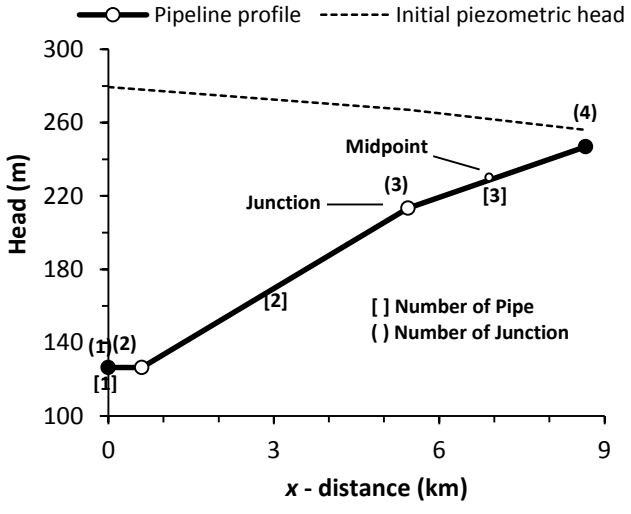


(a)

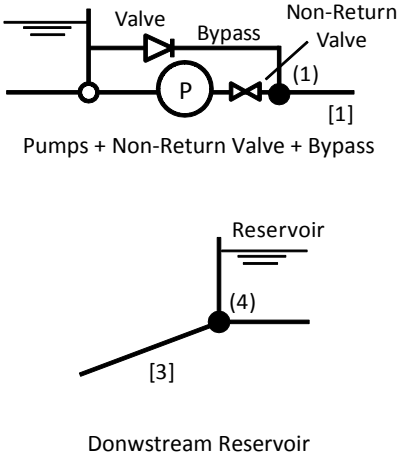


(b)

**Figure 2.** (a) System layout. (b) Schematic of some boundary conditions.

**Table 1:** Characteristics of the pipeline.

| Pipe number | $D$ (mm) | $L$ (m) | $f$ | $V_0$ (ms$^{-1}$) | $a$ (ms$^{-1}$) |
|---|---|---|---|---|---|
| [1] | 762 | 609.6 | 0.013 | 1.63 | 1,094.2 |
| [2] | 762 | 4,828.0 | 0.013 | 1.63 | 1,094.2 |
| [3] | 762 | 3,218.7 | 0.019 | 1.63 | 1,062.5 |

**Table 2:** nodes characteristics.

| Junction number | Type of Junction | Elevation $z$ (m) | $H$ (m) |
|---|---|---|---|
| (1) | Pump Discharge Point | 126.492 | 279.502 |
| (2) | Simple | 126.492 | 277.978 |
| (3) | Simple | 213.360 | 267.005 |
| (4) | Reservoir | 246.888 | 256.032 |

**Table 3:** pumps' characteristic curves (BHP = British Horse Power).

| $Q$ (L/s) | $H$/stage (m) | BHP/stage |
|---|---|---|
| 0.0 | 39.3 | 50.0 |
| 63.0 | 38.9 | 58.0 |
| 126.2 | 36.9 | 78.0 |
| 189.3 | 31.5 | 92.0 |
| 252.4 | 20.5 | 97.0 |
| 283.9 | 0.0 | 80.0 |

**Figures 3 and 4** show the pressure vs. time plot in junction 3 and in the midpoint of pipe 3, respectively, where it is possible to observe the following events sequence for the junction 3 (counted from the pumps shutdown time):

- **Time: 6.4 (s).** The pressure drops up to reach the vapor pressure $H_v$ whose value is approximately equal to –1 atmosphere (or –10.06 m gauge) in junction 3 and in midpoint of pipe 3. An air cavity is formed (**Figure 5**).
- **Time: 23.8 (s).** The air cavity collapses (**Figure 5**).
- **Time: 28.6 (s).** The first pressure peak of 135.0 (m) is generated.
- **Time: 39.7 (s).** A second pressure peak of 174.0 (m) is generated which is not caused by a second cavity collapse.
- **Time: 42.1 (s).** Pressure falls again to reach the vapor pressure without reaching to form an air cavity.
- **Time: 50.8 (s).** Again the pressure drops to reach the vapor pressure without reaching to form an air cavity.

Thereafter the minimum pressures tend to be positive and the effect of the pipe friction factor causes the pressures train tend to fade with over time.

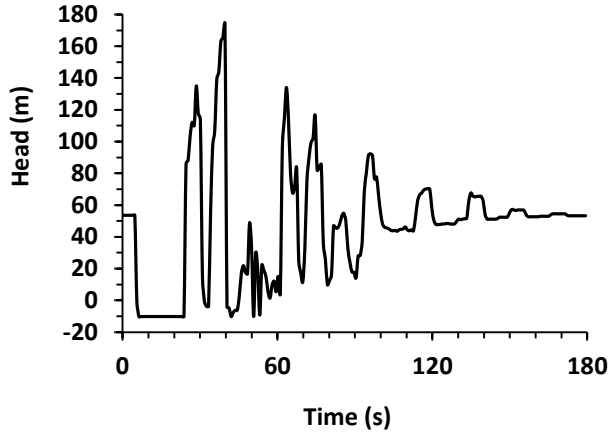


**Figure 3.** Pressure at the junction 3 ($N_1$ = 7).

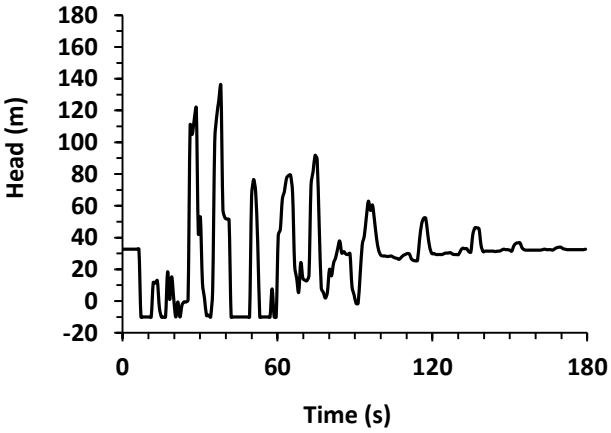


**Figure 4.** Pressure at the midpoint of pipe 3 ($N_1$ = 7).

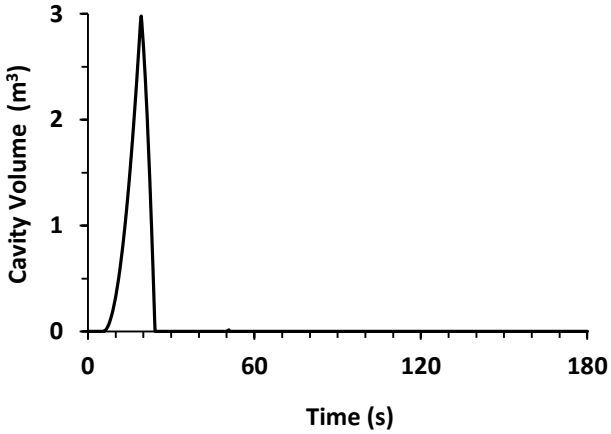


**Figure 5.** Air cavity volume at the junction 3 ($N_1$ = 7).

It is observed in **Figures 3 and 4** that the magnitude of the main pressure peak is lower than the maximum "expected" pressure according to the Joukowsky expression given by:

$$H^{max} = H_0 + \Delta H = H_0 + \frac{a \cdot Q_u}{2gA} \quad (9)$$

In this case $H^{max}$ = 390.0 (m) when the known values are replaced in (9). In **Figure 3**, adding the pipeline elevation, the maximum peak of the piezometric head (MPPH) is 387.4 m ($t$ = 39.6 s). In **Figure 4**, the MPPH is 365.5 m ($t$ = 38.1 s).

**4. Effect of the pipe discretization.**

Simpson and Bergant [14] and Tatu [16] emphasizes that numerical model of the cavity collapse must pay close attention to the way as network is discretized, especially in the spatial grid size ($\Delta x$). The coarse discretization generates greater $\Delta x$ value and, therefore, a higher theoretical cavity volume, whose numerical collapse could generate unrealistic pressure peaks. When $N_1$ = 1 in pipe 1 (the shortest one), $C_n$ = 1.00 and $\Delta t$ = 0.557103064 (s). The number of reaches ($N$) and $C_n$ for the rest of pipes are:

- Pipe 2: $N_2$ = 7, $C_n$ = 0.88.
- Pipe 3: $N_3$ = 5, $C_n$ = 0.92.

In this case the length of the pipe reaches ($\Delta x$) is:

- 
- Pipe 1: $\Delta x_1$ = 609.6 (m).
- Pipe 2: $\Delta x_2$ = 689.7 (m).
- Pipe 3: $\Delta x_3$ = 643.7 (m).

On the other hand, when pipe 1 is discretized using $N_1$ = 7, the length of $\Delta x$ is:

- Pipe 1: $\Delta x_1$ = 87.1 (m).
- Pipe 2: $\Delta x_2$ = 87.8 (m).
- Pipe 3: $\Delta x_3$ = 84.7 (m).

**Figures 6 and 7** show a comparison of the pressure evolution in junction 3 and in the midpoint of pipe 3, when $N_1$ is equal to 1 and 7.

**5. Sensitivity of DVCM results to input parameters.**

Another important aspect is the sensitivity of the numerical model results to changes of input parameters (wave speed, friction factor, pipe diameter; pipe slope, pipe length). According to Simpson and Bergant [14], a little wave speed variation may result in a large scatter of the maximum pressure expected value, especially in short pipelines. An investigation about the friction factor revealed that during transient cavitating flow the pipeline may operate in two regions depending on the friction factor size. Movement from one region to another occurs at a transition friction factor. For low friction factors the maximum pressure head is the short-duration pressure pulse that follows after the cavity collapse. The variations of the maximum pressure for changes in diameter are related to the resulting change in friction factor: as the diameter increases, the friction factor decreases, and depending on the case, the maximum pressure is governed by the Joukowsky pressure rise or by a short-duration pressure pulse following cavity collapse. For short pipelines an increase in negative slope leads to more severe vaporous cavitation along the pipeline therefore decreasing the maximum pressure of the short-duration pulses.

**6. Maximum length of the cavity.**

The maximum length of the cavity ($L_{vc}$) must be small compared to $\Delta x$, and both parameters must fulfill the following relationship for distributed cavitation regions [2]:

$$\frac{L_{vc}}{\Delta x} < 0.1 \quad (10)$$

Where $L_{vc} = V_v/A$, with $V_v$ = volume of the vapor cavity. If equation (10) is not fulfilled, then the DVCM model is not longer valid and the application of alternative models should be considered. Condition (10) may sometimes be violated since the water column separation is generally a local phenomenon where only a few grid points are affected [2]. For the analyzed example, the result shown in **Figure 8** is obtained, where it is observe that when $N_1$ varies between 1 and 9, the relation $L_{vc}/\Delta x$ is always less than 0.1. Thus, in this case we can conclude that the applied DVCM model is numerically valid. However, it is important to highlight that Wan et al. [19] proposed a 2D CFD model which has not restriction about cavity size in the simulations.

**7. Discussion.**

In **Figures 6 and 7** the $\Delta x$'s increase in magnitude meant an attenuation of the maximum peak pressure (10.2% in the first case, and 5.9% in the second case). This may be due in part to the Courant number effect because $\Delta x$'s increase did reduce their initial value, especially in pipes 2 and 3, although not significantly. Even though, as is expected the interpolation within the MOC grid causes numerical damping [6].

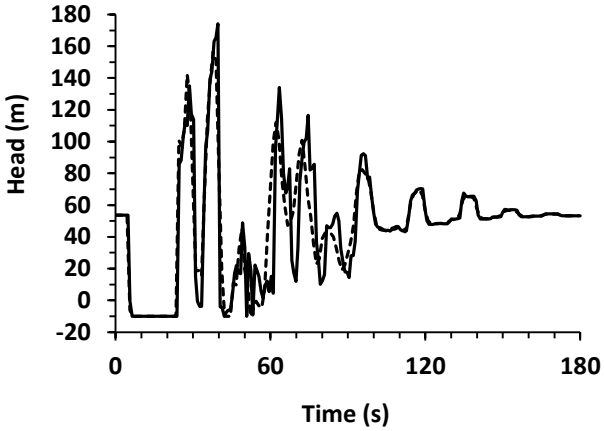


**Figure 6.** Pressure at the junction 3 when $N_1$ = 1 (continuous line) and when $N_1$ = 7 (dotted line).

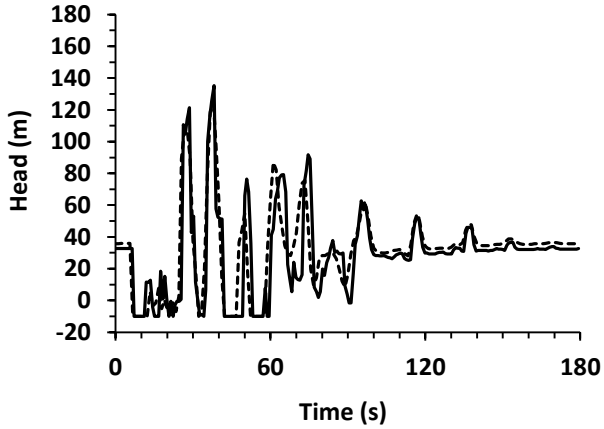


**Figure 7.** Pressure at the midpoint of pipe 3 when $N_1$ = 1 (continuous line) and when $N_1$ = 7 (dotted line). Note: in this case the location of the pipe's midpoint does not exactly match when $N_1$ = 1 and $N_1$ = 7.

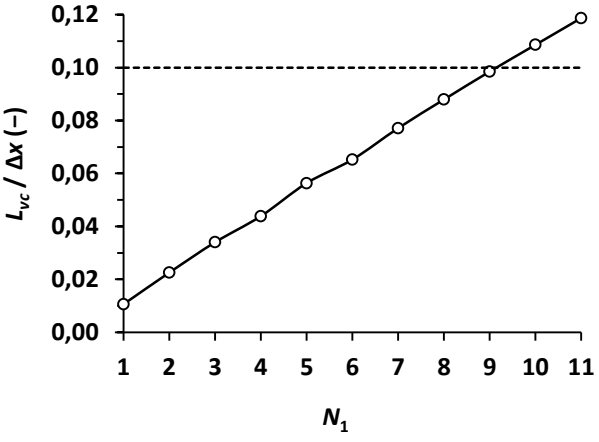


**Figure 8.** Relationship $L_{vc}/\Delta x$ in pipe 3.

Another aspect that could explain the difference when $N_1$ = 1 and $N_1$ = 7 is because of greater number of reaches, where the greater number of cavities which form along the pipeline during column separation tends to increasing the possibility of the random multi-cavity collapse. This result in a superposition of waves and in unrealistic pressure spikes [1, 14, 19]. Only in systems with clearly defined cavity positions the results are fairly realistic, at least through the first cavity collapse [20]. Another drawback of classical DVCM is that it cannot readily distinguish between localized vapor cavity formation and distributed cavitation, being necessary a combined model by considering local liquid column separations at high points and regions of distributed vaporous cavitation [19], all of which tends to complicate the analysis. On the other hand, Tatu [16] recognizes that the vapor cushion volume will depend on the number of the calculation nodes. The bigger is the number of the calculation nodes, the smaller is the vapor cushions volume concentrated in the computing nodes. So, the calculation results will depend on the number of the calculation nodes, so that the computing nodes number will have a great influence on the results, and only in very special cases the vapor volume will have a vapor cushion shape concentrated in a given point. Another relevant point which could explain the discrepancies it is that when the pressure at the internal computational section drops below the vapor pressure, the discharge at this section takes the average of the two discharges calculated from equations (3) and (4); because this averaging discharges has no physical meaning [2] it could be an error source.

## 8. Conclusions.

When the pressure falls up to reach the vapor pressure, cavities or bubbles will develop in the liquid. In the DVCM these cavities are concentrated at the grid points. Between the grid points, pure liquid is assumed for which the basic water hammer equations remain valid. This means that the pressure wave speed ($a$) is maintained between grid points in distributed cavitation regions. However, in bubble flow $a$ is both very low and pressure-dependent. Pressure waves actually do not propagate through an established distributed cavitation region, since this is at an assumed constant vapor pressure. The annihilation of a distributed cavitation region by a pressure wave causes a delay in propagation, which must be regarded as a wave speed reduction. In the DVCM the cavities, concentrated at grid points, do not move. This is consistent with the acoustic approximation: since the overall time scale is acoustic (water hammer), the vapor bubbles displacements are small. After the water column separation (WCS), the collision of two liquid columns, or of one liquid column with a closed end, moving towards the shrinking cavity, may cause a large and nearly instantaneous rise in pressure. The occurrence of liquid column separation may have a significant impact on subsequent transients in the system. Even though, the WCS modelling and subsequent cavity collapse requires the use of computational tools. The DVCM is the most commonly used model for column separation and distributed cavitation because it is easy to implement and it reproduces many physical events associated to the column separation in pipelines. Besides, the DVCM gives acceptable results only when the cavity occurs in a clearly and isolated defined position. One disadvantage of the DVCM is that multi-cavity collapse may produce unrealistic pressure spikes when the number of reaches becomes relatively large. For that reason, DVCM model gives reasonably accurate results when the number of reaches is restricted. Another disadvantage of the DVCM model is which in order to ensure a reliable result, in each analyzed case is necessary calculate the relationship $L_{vc}/\Delta x$ in order to know how discretize the network being necessary a trial/error procedure.

## 9. Acknowledgements.

Author express his gratitude to both Professor E. John List (chairman of Flow Science Incorporated) and his assistant, Mrs. Melinda Werts, for allowing a rapid access to the articles called “Sudden Pressure Drop and Pipeline Failure – Case Studies” (1994) and “Vapor Cavity Formation and Collapse: Field Evidence for Major Pipeline Damage” FEDSM99-6886 (1999).

## 10. References.

[1] Adamkowski A., Lewandowski M. (2009). A New Method for Numerical Prediction of Liquid Column Separation Accompanying Hydraulic Transients in Pipelines. *Journal of Fluids Engineering*, 131: 071302−1 − 071302−11.

[2] Bergant A., Simpson A.R., Tijsseling A.S. (2004). Water Hammer with Column Separation: A Review of Research in the Twentieth Century. *Centre for Analysis, Scientific Computing and Applications*, Department of Mathematics and Science, Eindhoven University of Technology. CASA Report: 04−34.

[3] Bergant A., Simpson A.R., Tijsseling A.S. (2006). Water hammer with Column Separation: A Historical Review. *Journal of Fluids and Structures*, 22: 135−171.

[4] Boulos P.F., Wood D.J., Lingireddy S. (2015). Shock and Water Hammer Loading. *Pressure Vessels and Piping Systems*. Encyclopedia of Life Support Systems (EOLSS), pp. 32.

[5] Collins R.P., Boxall J.B., Karney B.W., Brunone B., Meniconi S. (2012). How Severe Can Transients Be After a Sudden Depressurization? *Journal of AWWA*, E243−E251.

[6] Goldberg D.E., Wylie E.B. (1983). Characteristics Method using Time-Line Interpolations. *Journal of Hydraulic*

*Engineering*, 109(2): 670−683.

[7] Hatcher, T.M., Malekpour A., Vasconcelos J., Karney B.W. (2015). Comparing Unsteady Modeling Approaches of Surges Caused by Sudden Air Pocket Compression. *Journal of Water Management Modeling*, C392. DOI: 10.14796/JWMM.C392.

[8] List E.J. (1994). Sudden Pressure Drop and Pipeline Failure – Case Studies. Hydraulics of Pipelines Conference. Sponsored by the Pipeline Division/ASCE, June 12-15, 1994, Phoenix, Arizona.

[9] List E.J., Burnam J., Solbrig R., Hoggatt J. (1999). Vapor Cavity Formation and Collapse: Field Evidence for Major Pipeline Damage. Proceedings of the 3rd ASME/JSME Joint Fluids Engineering Conference, July 18-23, 1999, San Francisco, California, FEDSM99-6886, 1-10.

[10] Malekpour A., Karney B.W. (2011). Rapid Filling Analysis of Pipelines with Undulating Profiles by the Method of Characteristics. *International Scholarly Research Network* (ISRN), Applied Mathematics, Article ID 930460, pp. 16.

[11] Malekpour A. (2014). Analysis of Rapid Pipeline Filling including Column Separation & Entrapped Air Effects (Ph.D. Thesis). Toronto: University of Toronto.

[12] Pozos-Estrada O., Fuentes O.A., Sánchez A., Rodal E.A., de Luna F. (2017). Analysis on the Effects of Entrapped Air on Hydraulic Transients in Pumping Pipelines. *Revista Internacional de Métodos Numéricos para Cálculo y Diseño en Ingeniería*, 33(1-2): 79–89. http://dx.doi.org/10.1016/j.rimni.2015.11.002

[13] Ramezani L., Karney B. (2017). Water Column Separation and Cavity Collapse for Pipelines Protected with Air Vacuum Valves: Understanding the Essential Wave Processes. *Journal of Hydraulic Engineering*, 143(2): 04016083-1 - 04016083-13. DOI: 10.1061/(ASCE)HY.1943-7900.0001235.

[14] Simpson A.R., Bergant A. (1994). Numerical Comparison of Pipe-Column-Separation Models. *Journal of Hydraulic Engineering,* 120(3): 361−377.

[15] Simpson A.R., Wylie E.B. (1991). Large Water-Hammer Pressures for Column Separation in Pipelines. *Journal of Hydraulic Engineering*, 117(10): 1310−1315.

[16] Tatu G. (2004). Cavitation in Water-Hammer Calculation. *The 6th International Conference on Hydraulic Machinery and Hydrodynamics*, Timisoara, Romania, October 21−22, 549−552.

[17] Twyman J. (2016). Water Hammer in a Water Distribution Network. *XXVII Latin American Hydraulics Congress* (IAHR), Spain Water & IWHR (China), Lima, Peru, September 26-30, pp. 10.

[18] Twyman J. (2017). Water Hammer Analysis in a Water Distribution System. *Ingeniería del Agua*, 21(2): 87-102. https://doi.org/10.4995/Ia.2017.6389

[19] Wang H., Zhou L., Liu D., Karney B., Wang P., Xia L., Ma J., Xu C. (2016). CFD Approach for Column Separation in Water Pipelines. *Journal of Hydraulic Engineering*, 04016036-1 - 04016036-11. DOI: 10.1061/(ASCE)HY.1943-7900.0001171.

[20] Wang L., Wang F., Karney B., Malekpour A. (2017). Numerical Investigation of Rapid Filling in Bypass Pipelines. *Journal of Hydraulic Research*, 1-10. ISSN: 0022-1686. http://dx.doi.org/10.1080/00221686.2017.1300193

[21] Wylie B.E., Streeter V. (1978). *Fluid Transients*, p. 206. New York: McGraw–Hill International Book Company.